

# A General-Purpose Digital Pulse-Shape Discrimination Algorithm

M. Nakhostin

**Abstract**— Digital pulse-shape discrimination (PSD) systems are widely used to extract various kinds of information from the shape of output pulses of radiation detectors. Such systems replace the traditional analog PSD circuits with numerical algorithms running on a digital processor which makes them more flexible for implementing various PSD methods. However, the available digital PSD algorithms have been generally tailored to the characteristics of the concerned detectors which limits their general use. Here, for the purpose of building a general-purpose digital PSD module, we present a PSD algorithm that with minimum alterations can be used with a wide range of radiation detectors. Our approach is based on using the cosine similarity measure to quantify the variations in the shape of detectors' pulses with respect to the shape of a unit step pulse. The method is described in details, and the results of the test experiments with different types of radiation detectors, including a boron tetrafluoride (BF<sub>3</sub>) proportional counter, a liquid scintillation detector, and a high purity germanium (HPGe) detector are shown. The performance of the algorithm is also compared to that of the common rise-time discrimination method.

**Index Terms**— Digital Signal Processing; Pulse-Shape Discrimination; Semiconductor Detectors; Scintillation Detectors; Proportional Counters; Cosine Similarity

## I. INTRODUCTION

In many radiation detectors, the shape of output pulses carries important information that can be used to categorize an event beyond the energy deposition in the detector, and the time of occurrence of the event. The shape of pulses may carry information related to the type, range and interaction location(s) of particles, pulse pile-up and incomplete charge collection in the detector. The pulse-shape discrimination (PSD) systems provide such information by measuring the differences in the shape of pulses. The history of PSD systems goes back to the development of organic scintillation crystals, where in response to particles of different specific ionization, pulses of different decay-times are produced [1]. Since then, analog PSD systems have been extensively used with a variety of radiation detectors

such as organic and inorganic scintillation detectors [2, 3], gas-filled [4], silicon [5] and germanium detectors [6].

The recent developments in fast analog-to-digital converters (ADCs) and digital circuits, and their application to signals from radiation detectors, has produced new opportunities for the extraction of pulse-shape information from various types of radiation detectors. An advantage of digital systems is the possibility of multifunction operation that allows building a single versatile pulse processing module for extracting PSD information along with energy and timing information from a wide range of radiation detectors. However, while rather general-purpose algorithms for energy and timing measurements are available, the reported PSD algorithms that rely on the capabilities of digital realm, such as frequency analysis methods [7-9], least-square methods [10-12] and pattern recognition methods [13-15], need to be tailored to the characteristics of the concerned detectors. In this paper, we report on a high-performance and general-purpose digital PSD algorithm that with minimum alterations can be used with a wide range of radiation detectors. The paper is organized as follows: Section II describes the PSD method. Section III is dedicated to the experimental results, Section IV discusses the advantages of the method and Section V summarizes the paper.

## II. THE METHOD

### A. The cosine similarity

In computer science, a similarity measure is a function that quantifies the similarity between two objects, represented by vectors. The similarity measures have been widely used in various fields of digital technology like image analysis, language processing and text mining [16]. A list of various similarity measures can be found in Ref. [17]. The cosine similarity measure quantifies the similarity between two vectors  $x$  and  $y$ , by calculating the cosine of the angle between the two vectors:

$$\cos \theta = \frac{x \cdot y}{|x||y|} = \frac{\sum_{i=1}^p x_i y_i}{\sqrt{\sum_{i=1}^p x_i^2} \times \sqrt{\sum_{i=1}^p y_i^2}}, \quad (1)$$

where  $x \cdot y$  is a scalar product of the vectors,  $|x|$  and  $|y|$  are, respectively, the norm of the vectors,  $x_i$  and  $y_i$  are the elements of the vectors,  $p$  is the number of vectors' elements and  $\theta$  is the

This paragraph of the first footnote will contain the date on which you submitted your paper for review. This work was supported by the U.K. Science and Technology Facilities Council (STFC) under Grant ST/L005743/1.

M. Nakhostin is with the Department of Physics, University of Surrey, Guildford, Surrey, GU2 7XH, UK (e-mail: M.Nakhostin@surrey.ac.uk).

angle between the two vectors. The maximum similarity happens with  $\cos(\theta)=1$  for identical vectors and the maximum dissimilarity is between orthogonal vectors with  $\cos(\theta)=0$ .

### B. The PSD algorithm

The cosine similarity was initially used for the PSD of CdTe detectors by employing several peak-sensing ADCs [18]. It has been also used in digital domain for the discrimination of neutrons and  $\gamma$ -rays with liquid scintillation detectors [19], and recently, for the correction of time-walk error in pulse timing with CdTe detectors [20]. In all these attempts, the cosine similarity was calculated between the sampled pulses and a pulse template from the concerned detector. In our PSD approach, the cosine similarity is calculated between the sampled pulses from a charge-sensitive preamplifier and a common unit step pulse, thereby no actual pulse template is required. The details of the PSD procedure are illustrated in Fig. 1. First, a digital discriminator, such as leading-edge or a constant-fraction discrimination (CFD) [21], marks the start of the pulse. Then, the vector  $x$  is formed by taking the pulse samples that lie in a time window starting from the pulse's start-time. The time window can have either a fixed length or a variable length. In the latter case, the time window for each pulse ends at a fixed fraction of the pulse amplitude, e.g. 90 % of the pulse's amplitude. The vector  $y$  is formed by taking the corresponding samples from a unit step pulse, as shown in the bottom of Fig. 1. This vector will be a vector of the same length as the vector  $x$ , with its elements all equal to unity. The choice of a fixed or variable time window is determined by the type of the detector. For ionization-type detectors in which the charge collection time can significantly vary from event to event, a variable time window is used, but for scintillation detectors in which the variations in the duration of pulses is insignificant, a fixed length time window is used.

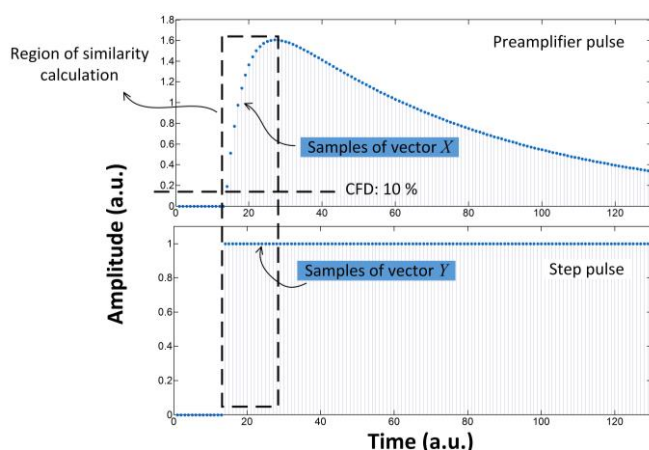


Fig. 1. The calculation of the cosine similarity PSD parameter for output pulses from a charge-sensitive preamplifier. The cosine similarity is calculated between vector  $x$ , composed of the samples in a time window in the leading-edge of the pulse, and vector  $y$ , composed of the corresponding samples from a simple unit step pulse. The start of the time window is determined by using a digital trigger. The length of the time window can be fixed, or end when the pulse reaches to a certain fraction of its amplitude.

### C. Analysis of the PSD method

When the cosine similarity of a detector pulse  $x$  is calculated against a simple unit step pulse  $y$ , since all the elements of the vector  $y$  are equal to unity, Eq. 1 is simplified to:

$$\cos \theta = \frac{\sum_i^p x_i}{\sqrt{p} \sqrt{\sum_i^p x_i^2}}, \quad (2)$$

where  $x_i$  denotes the  $i$ th sample of the sequence, and  $p$  is the number of the samples in the time window. The numerator of this relation, the sum of signal samples, simply gives the area under the signal waveform which has been already used in the calculation of the PSD measure in the classic charge-comparison method. In the denominator, the sum of square of the signal's samples gives the signal's power, which is again a function of the pulse-shape characteristics. Indeed, the signal power has been already used in the PSD of neutrons and  $\gamma$ -rays with organic scintillation detectors [8, 22, 23]. If a variable time window is employed, then the term  $p$  can be also set to reflect the rise-time of the pulse. Therefore, our cosine similarity PSD approach is sensitive to different types of differences in the shape of detectors' pulses. While in PSD applications one aims at measuring the deterministic variations in the shape of pulses, these variations can be masked under the random variations in the shape of the pulses. In scintillation detectors such random variations mainly originate from the discrete nature of photoelectrons emission. In ionization-type detectors, the random variations mainly originate from the electronic noise. The performance of any PSD system will depend on how sensitive the method is to the deterministic pulse-shape variations and how resistive the method is against the random variations. If the pulse-shape characteristics and the nature of random variations are known, an optimum PSD system can be designed, as it was reported by Gatti for organic scintillation detectors [24]. Eq. 2 indicates that the cosine similarity method is sensitive to various types of deterministic variations in the shape of pulses which makes it a suitable general-purpose PSD method, but it cannot be the optimum method for all types of detectors due to the different nature of random variations in different types of detectors. However, it has been shown in some studies that among various distance measures the Euclidean distance, which is equivalent to the calculation of the cosine similarity of normalized vectors, is optimal in presence of white Gaussian noise [25].

## III. EXPERIMENTAL RESULTS

The PSD algorithm was examined with three different types of detectors, including a  $\text{BF}_3$  proportional counter (40 cm long and 1.5 cm diameter, from LND, USA), a cylindrical BC501A liquid scintillation detector (5 cm long and 5 cm diameter) coupled to a photomultiplier tube of type 9266B (Electron Tubes, UK), and a closed-end coaxial HPGe detector (5.15 cm long and 5.05 cm diameter, from Canberra, USA). The output signals from all the detectors were readout with charge-sensitive preamplifiers and directly fed into a waveform digitizer with a maximum sampling frequency of 4 GHz and

10-bit resolution (model DC252HF from Agilent Technologies Inc). The detectors' signals were sampled event-by-events and stored to a hard disk drive for offline analysis by using a program written in MATLAB language. The digital pulse processing was comprised of calculating the cosine similarity PSD parameter and the energy of each event. The same procedure for the calculation of the cosine similarity PSD is applied to pulses from all the examined detectors, with a fixed time window for the liquid scintillation detector and a variable window for the  $\text{BF}_3$  and HPGe detectors. For comparison purposes, the signal power PSD method and the rise-time discrimination method (two components of Eq. 2) were also implemented. The signal power PSD parameter was calculated as the sum of square of the pulse samples, normalized to the pulse's amplitude. The rise-time was calculated by using two digital CFDs. The PSD information were extracted by depicting the PSD parameters against the events' energy which is reflected in the amplitude of the pulses. In the case of the liquid scintillation detector, the common term *light output* is used to express the energy deposition in the detector. The pulse processing steps for the measurement of the amplitude of the pulses involved a digital baseline correction followed by a digital semi-Gaussian pulse shaper [26] to minimize the effect of the electronic noise.

#### A. The $\text{BF}_3$ neutron detector

Proportional counters filled with  $\text{BF}_3$  or  $^3\text{He}$  gases are commonly used for the detection of slow neutrons in various applications such as neutron scattering experiments, health physics, and nuclear safeguard. The digital PSD methods have been used with these detectors for purposes such as study on the direction of the ionization track of neutron absorption reaction products [27, 28], rejection of spurious and background events [29, 30], and improvement of the discrimination between neutrons and  $\gamma$ -rays [31]. The digital PSD algorithms used in these applications were the charge-comparison method [27], the rise-time discrimination method [28], and the pulse-width measurement method [27]. The use of pattern recognition methods including the principle component analysis and the

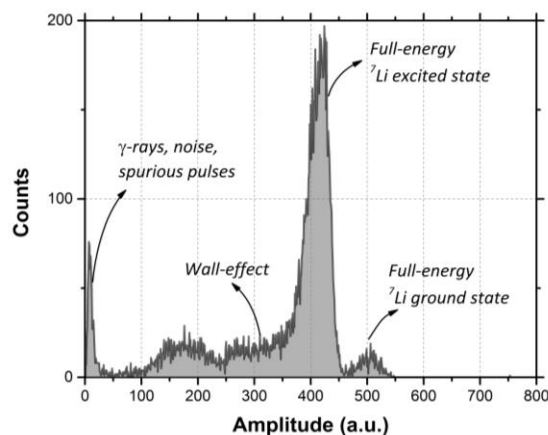


Fig. 2. The pulse-amplitude distribution of the  $\text{BF}_3$  neutron detector. The detector was operated with 1470 volt. The distribution was obtained by digital processing of the detector's pulses, sampled at 250 MHz. The shaping time constant of the digital pulse shaper was 3.5  $\mu\text{s}$ . The peaks, the wall-effect continuum and the unwanted events including  $\gamma$ -rays, noise and spurious pulses are indicated.

Fisher's linear discriminant analysis were also reported in Ref. [31].

Fig. 2 shows the pulse-amplitude distribution of the  $\text{BF}_3$  neutron detector exposed to thermalized neutrons from an Am/Be neutron source. The pulse-amplitude distribution has two peaks: a large one ( $^7\text{Li}$  left in an excited state) and a small one ( $^7\text{Li}$  left in the ground state). The wall-effect, which occurs when one of the neutron absorption reaction products hits the detector's wall, is also seen in the distribution. The  $\gamma$ -ray events together with other unwanted events such as noise and spurious events from electric discharges in the detector appear at the low energy range. Although a simple amplitude discrimination is generally sufficient to discriminate neutron events against the unwanted events, there exist applications with a requirement on

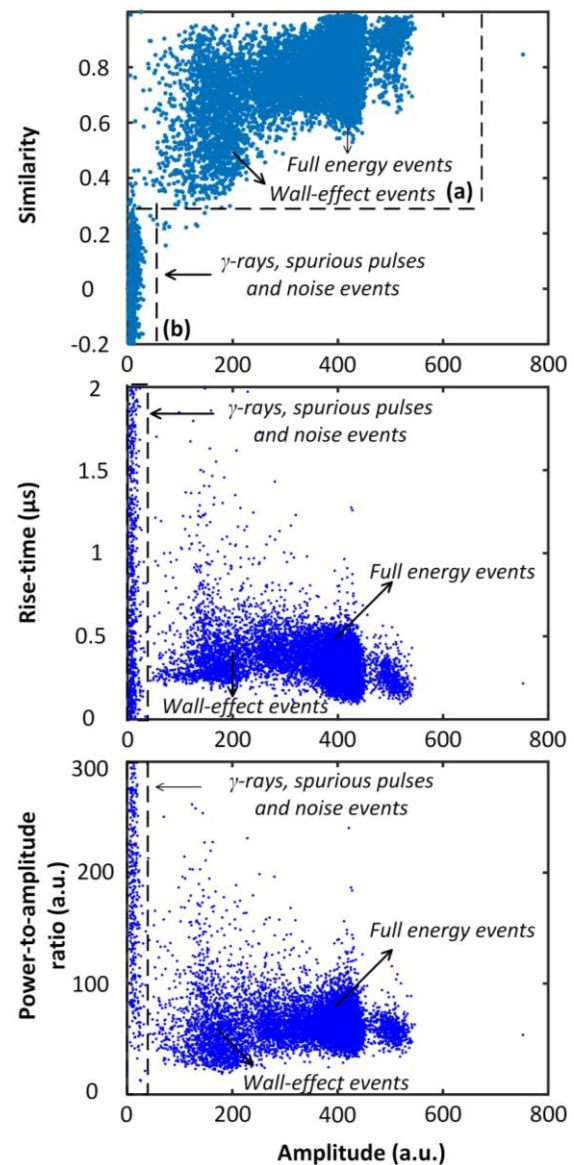


Fig. 3. (Top) The cosine similarity PSD parameter against the pulse amplitude for events from the  $\text{BF}_3$  neutron detector. (Middle) The PSD results of the rise-time discrimination method. The rise-time was calculated from 10 % to 90 % of the pulses' amplitude. No filter was applied to the pulses prior to the rise-time measurements. (Bottom) The PSD results of the signal power method. A clear separation of the neutron events against the unwanted events is achieved by using the cosine similarity PSD method. The number of analysed pulses was 36000.



a neutron to  $\gamma$ -ray discrimination ratio of above  $10^6$  that necessitates the combination of pulse amplitude and pulse-shape discrimination methods [32].

Fig. 3 shows the results of the cosine similarity PSD method for the  $\text{BF}_3$  neutron detector. The PSD parameter was calculated by using a variable time window from 10 % to 90% of each pulse's amplitude. For comparison purposes, the results of the rise-time discrimination and signal power PSD methods are also shown. The scatter plot of the cosine similarity against the pulse amplitude shows two distinctive regions: (a) genuine neutron events; (b) unwanted events due to  $\gamma$ -rays, noise, and spurious pulses. It is apparent that, compared to the rise-time discrimination and the signal power methods, a much better separation of the neutron events from other events is achieved with the cosine similarity PSD method. The orientation of particles' track is also well reflected in the cosine similarity PSD parameter: the wall-effect events exhibit smaller similarity than the full-energy deposition events. The reflection of the orientation of the ionization track of neutron absorption reaction products on the PSD parameter of pulses is further shown in Fig. 4. One can see that, for the full-energy deposition events, an amplitude deficit happens as the similarity decreases. This is due to the fact that as the ionization track approaches to the direction normal to the anode wire, the space-charge effect of positive ions increases, that in turn, suppresses the gas amplification process [28].

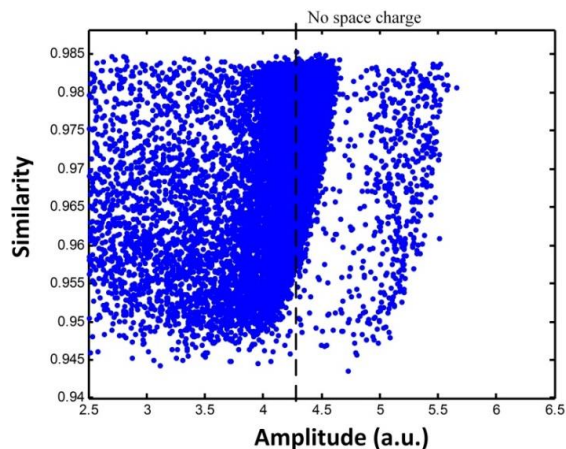


Fig. 4. The reflection of the space-charge effect on the cosine similarity PSD parameter of pulses. For the full-energy deposition events, a smaller PSD parameter indicates that the direction of ionization track approaches to the direction normal to the anode wire. The consequent reduction in the electric field due to the space-charge effect results in a reduction in the pulse amplitudes.

### B. Liquid scintillation detector

A large number of digital PSD algorithms have been proposed for the discrimination of fast neutrons against  $\gamma$ -rays in liquid scintillation detectors. Some of these algorithms include the digital versions of the classic analog charge-comparison and the zero-crossing methods [33, 34], pulse gradient analysis [35] and frequency domain methods [7-9]. There have been also some efforts on the utilization of machine learning methods including artificial neural networks [36],

support vector machine [37], Bayes' theorem [38] and fuzzy c-means [39]. Fig. 5 shows the results of different PSD methods for the BC501A liquid scintillation detector exposed to an Am/Be neutron source. All the PSD methods are applied to the output pulses of an integrating preamplifier, where the information on the type of particles is reflected in the leading-edge of the pulses. The PSD parameters are shown as function of the amplitude of the pulses, calibrated to scintillation light output in units of electron-equivalent energy (keVee) by using standard laboratory  $\gamma$ -ray sources. The cosine PSD parameter was first calculated through Eq. 2 and for a fixed time window of 180 ns, starting from 10 % of a pulse's amplitude. One can see that the neutron and  $\gamma$ -rays distribute themselves in different regions. The events in the lower plume are neutrons and the events in the higher plume are  $\gamma$ -rays, as their steeper leading-edge makes them more similar to a step pulse. Since for liquid scintillation detectors neutron and  $\gamma$ -ray pulse templates are known [11], it is worthwhile to study the performance of the cosine similarity PSD method when the similarity is calculated against an actual pulse template instead of a simple step pulse.

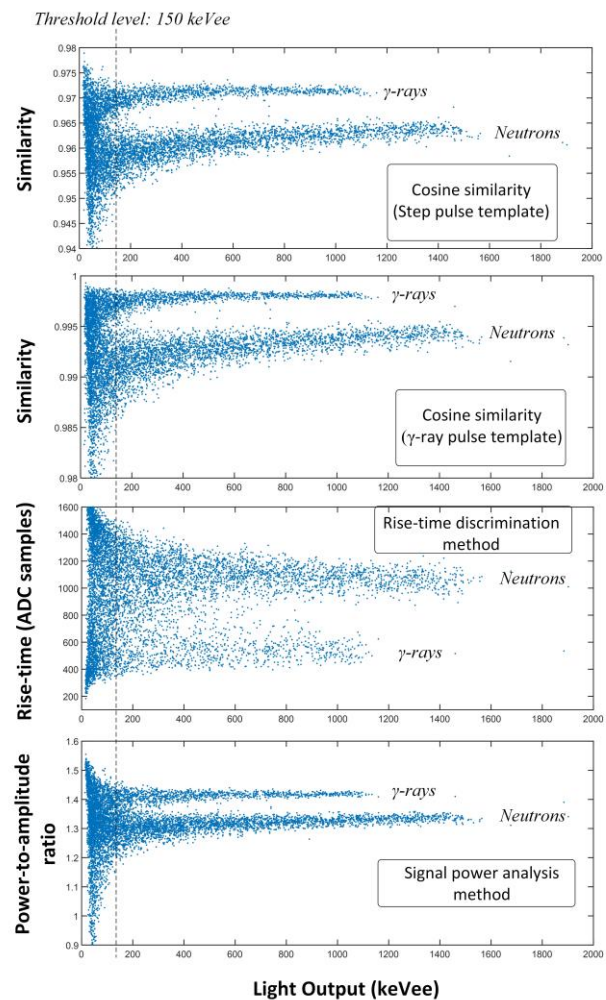


Fig. 5. The results of neutron and  $\gamma$ -ray discrimination by using the cosine similarity method, calculated against a simple step pulse and a  $\gamma$ -ray pulse template, as well as the results of the rise-time discrimination and the signal power analysis methods. The cosine similarity was calculated for a fixed time window of 180 ns. The detector pulses were sampled at a sampling frequency of 4 GHz. The optimum rise-time measurement window was found to be from 10 % to 95 % of a pulse's amplitude.

We calculated the cosine PSD parameter against a  $\gamma$ -ray pulse template as reported by Marrone *et al.* [11]. The PSD results together with the results of the rise-time discrimination and signal power analysis PSD methods are also shown in Fig. 5. By assuming Gaussian distributions for the PSD parameters, the PSD methods can be quantitatively compared by computing a figure-of-merit (FOM), defined as:

$$FOM = \frac{S}{FWHM_{\gamma} + FWHM_n}, \quad (3)$$

where  $S$  is the distance between the  $\gamma$ -ray and neutron peaks in the histogram of the PSD parameter, and  $FWHM_n$  and  $FWHM_{\gamma}$  are the full-width at half-maximum of the neutron and  $\gamma$ -ray peaks. The results of the FOM calculations for events in the light output range of 150-1600 keVee are shown in Fig. 6, which depicts the projections of the scatter plots of Fig. 5 upon the vertical axis. The FOMs were calculated by fitting a double Gaussian function to the PSD spectra. A FOM value of  $1.38 \pm 0.08$  was achieved with our cosine similarity PSD method against  $FOM = 1.29 \pm 0.04$  for the cosine similarity method by

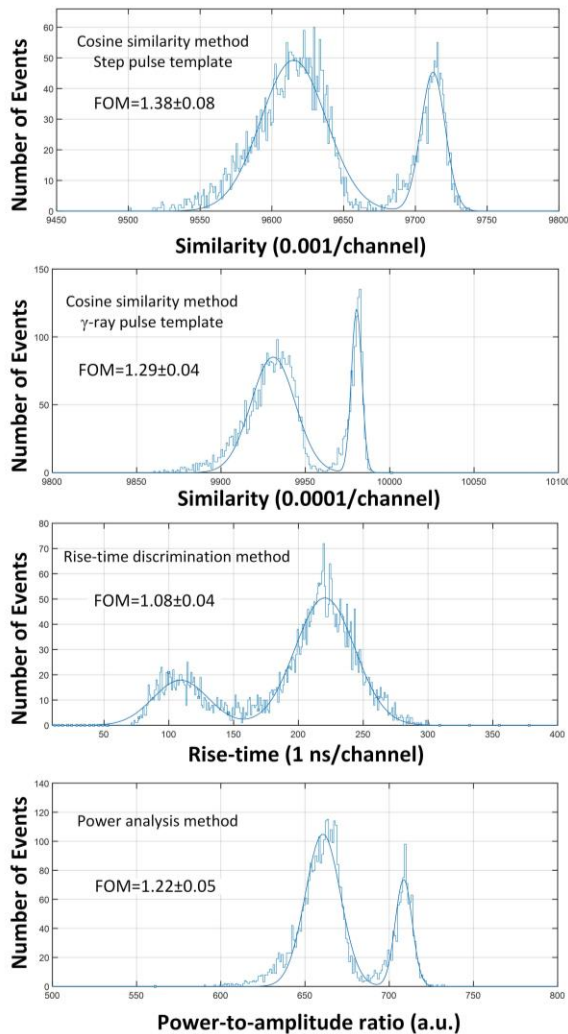


Fig. 6. The results of FOM calculations for the cosine similarity PSD method by using a simple step pulse and by using a  $\gamma$ -ray pulse template, as well as the results of the rise-time discrimination and the signal power analysis PSD methods. The light output range was 150-1600 keVee.

using a  $\gamma$ -ray pulse template,  $FOM = 1.08 \pm 0.04$  for the rise-time discrimination method and  $FOM = 1.22 \pm 0.04$  for the signal power analysis method. These results show that by using an actual detector pulse template the performance of the cosine similarity method does not improve. The cosine similarity method by using a simple step pulse also outperforms the rise-time discrimination and the signal power analysis PSD methods.

### C. HPGe detector

Digital PSD of HPGe detectors has been extensively studied for purposes such as Compton suppression [40], background rejection in double beta-decay experiments [41], correcting for the effect of radiation damage [42],  $\gamma$ -ray tracking with segmented electrode detectors [43], and detection of fast neutrons [44]. The digital PSD methods used with germanium detectors include measurement of the time-to-peak of current pulses [40], calculation of the ratio of the amplitude of current pulses to the events' energy [43], and comparison of pulse shapes to a basis data set [42]. For closed-end coaxial germanium detectors, the PSD methods have been mainly studied for the purpose of Compton suppression [40]. In germanium detectors, the variations in the shape of pulses mainly result from the variations in the interaction locations and the number of interactions in the crystal. For our 5.15 cm by 5.05 cm germanium crystal, a  $\gamma$ -ray in the energy range 200 keV to a few MeV, will usually Compton scatter 2-4 times before

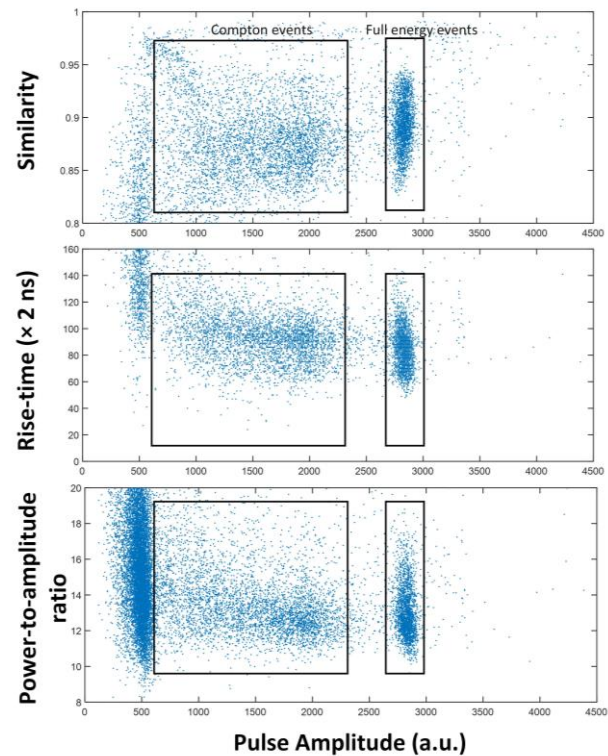


Fig. 7. (Top) The scatter plot of the cosine similarity PSD parameter as a function of the pulse amplitude. (Middle) The rise-time of the events as a function of the pulse amplitude. (Bottom) The signal power PSD parameter as a function of the pulse amplitude. The results are shown for  $\gamma$ -rays from  $^{137}\text{Cs}$ . The detector's pulses were sampled at 500 MHz and the shaping time constant of the digital shaper was 1  $\mu\text{s}$ .

full energy deposition [45]. This leads to multi-site pulses whose shape is a linear sum of the pulses produced at each interaction site (with each term weighted by its respective energy deposition). Since single-site events are more likely to be a Compton scatter event, the difference in the pulse-shape characteristics of multi-site and single-site events may be used to achieve some degree of Compton suppression. Fig. 7 shows the results of the cosine similarity, rise-time discrimination and signal power PSD methods for the HPGe detector exposed to a  $^{137}\text{Cs}$   $\gamma$ -ray source. The cosine similarity PSD parameter was calculated for a variable time window from 10 % to 90 % of each pulse's amplitude. In principle, the possibility of suppressing the Compton events by using a PSD technique depends on the existence of a difference in the distributions of the PSD parameter for the Compton scattered events and the full-energy events. Fig. 8 shows the distributions of the PSD parameters for the two groups of the full-energy events and the Compton scattered events from the regions shown in Fig. 7. The distributions are normalized to the total number of events. The distributions do not strictly follow a Gaussian shape as the shape is a function of the type of PSD measure and the distribution of the interaction locations of  $\gamma$ -rays in the detector. The difference between the distributions of the PSD parameter of the two groups of events was evaluated by calculating the non-overlap area between the two distributions. It was found that for the cosine similarity PSD method the non-overlap area contains 32.54 % of the total number of events against 20.98 %

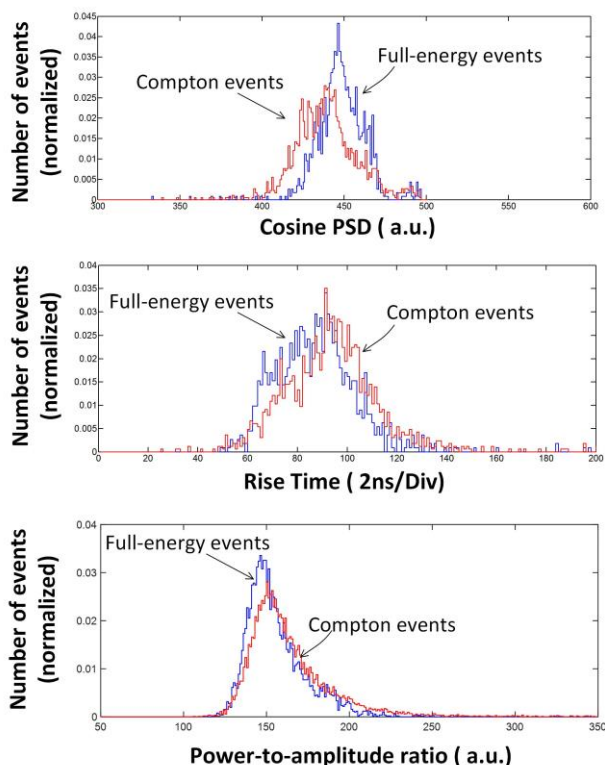


Fig. 8. (Top) A comparison of the distributions of the cosine similarity PSD parameter for the full energy events and the Compton scattered events from the regions shown in Fig. 7. The non-overlap region is 32.54 % of the total number of events. (Middle) The rise-time distribution of the full-energy and the Compton scattered events. The non-overlap region is 20.98 % of the total number of events. (Bottom) The distribution of the signal power PSD parameter for the full energy and Compton scattered events. The non-overlap region is only 14.17 % of the total number of events.

for the rise-time discrimination method, which is understandable because single-site events and multi-site events can have the same rise-time but different time profiles [44] that leads to different cosine similarity PSD parameters. The non-overlap area is only 14.17 % for the signal power analysis PSD method.

As a test of Compton suppression by using the cosine similarity PSD parameter, a measurement of  $\gamma$ -rays from  $^{137}\text{Cs}$ ,  $^{60}\text{Co}$  and  $^{22}\text{Na}$  was taken. The detector was very briefly exposed to the  $^{22}\text{Na}$  source so that the 511 keV  $\gamma$ -ray peak almost lies under the Compton continuum of higher energies. Fig. 9 shows the original pulse-amplitude distribution and the distribution after rejecting the events with a typical cosine similarity below 0.89. As a result of the rejection of these events, some of the Compton scattered events together with some of the full energy events are lost but the net result is an improvement in the peak-to-Compton ratio. It is seen that the 511 keV peak clearly stands out of the Compton background. The improvement was quantified by fitting a Gaussian function to the 511 keV peaks. The peak-to-Compton ratio defined as the number of events in the peak channel to the number of events at the channel three standard deviations below the peak channel improves from 1.01 to 2.11 for this particular example.

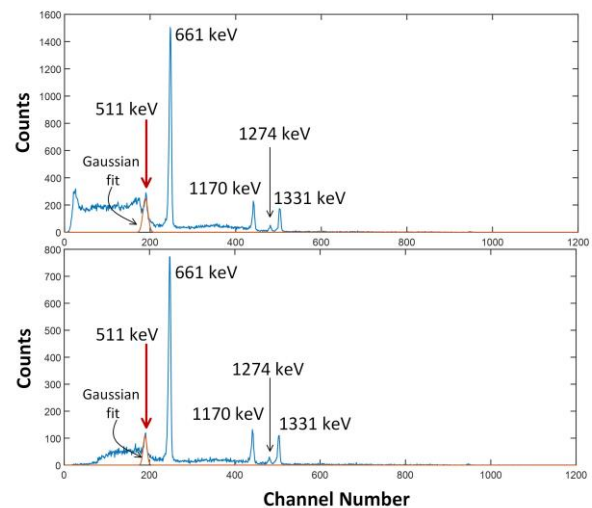


Fig. 9. (Top) The original pulse-amplitude distribution of  $\gamma$ -rays from  $^{137}\text{Cs}$ ,  $^{60}\text{Co}$  and  $^{22}\text{Na}$ . (Bottom) The pulse-amplitude distribution after rejecting the events with a cosine similarity below 0.89. The 511 keV peak stand above the Compton continuum.

#### IV. DISCUSSION

The cosine similarity measure exhibits several attractive features for PSD applications of radiation detectors. One important feature is that the cosine similarity is a measure of the orientation and not the magnitude, and thus, it solely reflects the pulse-shape information, regardless of the amplitude of the pulses. In fact, most of the available similarity/distance measures are dependent on the magnitude of the vectors, and thus, their use for PSD applications requires to first normalize the preamplifier pulses to their amplitudes. Since preamplifiers' pulses are generally quite noisy, the normalization process can



cause a significant error in the extraction of the pulse-shape information. The second advantage of the cosine similarity PSD method is that it does not require the production of an actual detector pulse template. Also, in comparison to the feature extraction pattern recognition PSD methods such as the principal component analysis and the Fisher's linear discriminant analysis methods [15, 30], this algorithm does not require training sets and a prior analysis of the detector's pulse-shape characteristics. Finally, the cosine similarity can be implemented with relatively small amount of computations that is important for real-time applications. Indeed, the cosine similarity measure has been already implemented on the field programmable gate arrays (FPGAs) with respect to different applications (see e.g. Refs. [46, 47]).

## V. SUMMARY AND CONCLUSION

We have studied the use of the cosine similarity measure as a general-purpose PSD algorithm of radiation detectors. It was shown that this algorithm is equivalent to the combination of three independent PSD methods of rise-time discrimination, charge-comparison and signal power analysis, which makes it applicable to a range of detectors of different pulse-shape characteristics. Data sets of pulses were collected from three different types of radiation detectors to extract the pulse-shape information, and the PSD results were compared against those of the common rise-time discrimination method as a common general-purpose analog PSD method, and the signal power analysis method as a component of the cosine similarity PSD method. It was found that the cosine similarity PSD method outperforms the rise-time discrimination and signal power PSD methods by providing accurate PSD information with the three different types of gas-filled, scintillation and semiconductor detectors. These results are very encouraging for building a versatile PSD system that can be used with different types of radiation detectors and suggest useful directions for future work, including studies with more detectors, examining the algorithm to see its performance against noise and sampling rate and starting to develop FPGA implementations.

## REFERENCES

- [1] R. B. Owen, "The decay times of organic scintillators and their application to the discrimination between particles of differing specific ionization," *IRE Transactions on Nuclear Science* 1958, Volume: 5, Issue: 3, Pages: 198 – 201.
- [2] F. D. Brooks, "A scintillation counter with neutron and gamma-ray discriminators," *Nucl. Instrum. and Meth.* 4 (1959) 151.
- [3] C. M. Bartle, "A study of (n,p) and (n, $\alpha$ ) reactions in NaI(Tl) using a pulse-shape-discrimination method," *Nucl. Instrum. and Meth. A* 124 (1965) 547.
- [4] E. Mathieson, and T. J. Harris, "Pulse shape discrimination in proportional counters - theory of electronic system," *Nucl. Instrum. and Meth. A* 88 (1970) 181.
- [5] G. Pausch, *et al.*, "Identification of light charged particles and heavy ions in silicon detectors by means of pulse-shape discrimination," *IEEE Trans. Nucl. Sci.* 43 (1996) 1097.
- [6] S. M. Hinshaw and D. A. Landis, "A practical approach to ballistic deficit correction," *IEEE Trans. Nucl. Sci.* 37 (1990) 374.
- [7] S. Yousefi and L. Lucchese, "A wavelet-based pulse shape discrimination method for simultaneous beta and gamma spectroscopy," *Nucl. Instrum. and Meth. A* 599 (2009) 66.

- [8] G. Liu, *et al.*, "A digital method for the discrimination of neutrons and gamma rays with organic scintillation detectors using frequency gradient analysis," *IEEE Trans Nucl. Sci.* 57 (2010) 1682.
- [9] M. J. Safari, *et al.*, "Discrete Fourier transform method for discrimination of digital scintillation pulses in mixed neutron-gamma fields," *IEEE Trans. Nucl. Sci.* 63 (2016) 325.
- [10] J.E. McFee, *et al.*, "Comparison of model fitting and gated integration for pulse shape discrimination and spectral estimation of digitized lanthanum halide scintillator pulses," *Nucl. Instrum. and Meth. A*, Vol. 828 (2016) 105.
- [11] S. Marrone, *et al.*, "Pulse shape analysis of liquid scintillators for neutron studies," *Nucl. Instrum. and Meth. A* 490 (2002) 299.
- [12] H. Semmaoui, *et al.*, "Crystal identification based on recursive-least-squares and least-mean-squares auto-regressive models for small animal PET," *IEEE Trans. on Nucl. Sci.* Vol. 55 (2008) 2450.
- [13] A. Dutta, K. E. Holbert, "Discrimination of neutron-gamma ray pulses with pileup using normalized cross correlation and principal component analysis," *IEEE Trans. on Nucl. Sci.*, Vol. 63 (2016) 2764.
- [14] T. S. Sanderson, *et al.*, "Machine learning for digital pulse shape discrimination," *IEEE Nuclear Science Symposium and Medical Imaging Conference Record* (2012) 199.
- [15] C. L. Wang, *et al.*, "Improved neutron-gamma discrimination for a  $^3\text{He}$  neutron detector using subspace learning methods," *Nucl. Instrum. and Meth. A* Vol. 853 (2017) 27.
- [16] P.-N. Tan, M. Steinbach, V. Kumar, "Introduction to Data Mining," Addison-Wesley (2005).
- [17] S. Cha, "Comprehensive survey on distance/similarity measures between probability density functions," *Int. Journal of Mathematical Models and Methods in Applied Science*, Vol. 1 (2007) 300.
- [18] Y. Takenaka, *et al.*, "Novel pulse-shape-analysis method by using similarity," *Appl. Radiat. Isot.* 49 (1998) 1219.
- [19] D. Takaku, *et al.*, "Development of neutron-gamma discrimination technique using pattern-recognition method with digital signal processing," *Progress in Nucl. Sci. and Technology*, Vol. 1 (2011) 210.
- [20] M. Nakhostin, "Optimizing timing performance of CdTe detectors for PET," *Physics in Medicine and Biology* 62 (2017) N485.
- [21] M. Nakhostin, T. Oishi, M. Baba, "Time resolution measurement of avalanche counters using digital signal processing technique," *Radiation Measurements*, 43 (2008) 1493.
- [22] D. I. Shippen, *et al.*, "A wavelet packet transform inspired method of neutron-gamma discrimination," *IEEE Trans. Nucl. Sci.* Vol. 57 (2010) 2617.
- [23] X. L. Luo, "Neutron/gamma discrimination employing the power spectrum analysis of the signal from the liquid scintillator BC501A," *Nucl. Instrum. and Meth. A* 717 (2013) 44.
- [24] E. Gatti, and F. De Martini, "A new linear method of discrimination between elementary particles in scintillation counters," in *Nuclear Electronics*, published by IAEA, Vol. 2 (1962) 265.
- [25] D. Francois, V. Wertz and M. Verleysen, "Non-Euclidean metrics for similarity search in noisy datasets," *Proceedings of European Symposium on Artificial Neural Networks, Burges (Belgium)*, April 2005, 339-344.
- [26] M. Nakhostin, "Recursive algorithms for real-time digital CR-(RC) pulse shaping," *IEEE Trans. on Nucl. Sci.*, Vol. 58 (2011) 2378.
- [27] H. Takahashi, *et al.*, "Digital signal processing for  $^3\text{He}$  proportional counters," *Nucl. Instrum. and Meth.* A353 (1994) 164.
- [28] N. Takeda and K. Kudo, "Influence of direction of charged particles produced by thermal neutrons on pulse height in  $^3\text{He}$  proportional counters," *IEEE Trans. on Nucl. Sci.*, Vol. 42 (1995) 548.
- [29] L. Chen, *et al.*, "Digital beta counting and pulse-shape analysis for high-precision nuclear beta decay half-life measurements: tested on  $^{26}\text{Al}^{\text{m}}$ " *Nucl. Instrum. and Meth. A* 728 (2013) 81.
- [30] T. J. Langford, *et al.*, "Event identification in  $^3\text{He}$  proportional counters using risetime discrimination," *Nucl. Instrum. Meth. A* 717 (2013) 51.
- [31] C. L. Wang, *et al.*, "Improved neutron-gamma discrimination for a  $^3\text{He}$  neutron detector using subspace learning methods," *Nucl. Instrum. and Meth. A* 853 (2017) 27.
- [32] Oak Ridge National Laboratory, Neutron Instrumentation, <http://neutrons.ornl.gov/instruments>.
- [33] Y. Kaschucka, B. Esposito, "Neutron/ $\gamma$ -ray digital pulse shape discrimination with organic scintillators," *Nucl. Instrum. and Meth.* 551 (2005) 420.
- [34] M. Nakhostin, P.M. Walker, "Application of digital zero-crossing technique for neutron-gamma discrimination in liquid organic scintillation detectors," *Nucl. Instrum. and Meth. A*, Vol. 621 (2010) 498.

- [35] B. D'Mellow, *et al.*, "Digital discrimination of neutrons and  $\gamma$ -rays in liquid scintillators using pulse gradient analysis," *Nucl. Instrum. and Meth. A*, Vol. 578 (2007) 191.
- [36] G. Liu, *et al.*, "An investigation of the digital discrimination of neutrons and  $\gamma$  rays with organic scintillation detectors using an artificial neural network," *Nucl. Instrum. Meth. A* 607 (2009) 620.
- [37] D. Savran, *et al.*, "Pulse shape classification in liquid scintillators using the fuzzy c-means algorithm" *Nucl. Instrum. Methods Phys. Res. A* 624 (2010) 675.
- [38] M. Monterial, *et al.*, "Application of Bayes' theorem for pulse shape discrimination," *Nucl. Instrum. Methods Phys. Res. A* 795 (2015) 318.
- [39] X. Yu, *et al.*, "Neutron–gamma discrimination based on the support vector machine method," *Nucl. Instrum. Methods Phys. Res. A* 777 (2015) 80.
- [40] G. J. Schmid, *et al.*, "HPGe Compton suppression using pulse shape analysis," *Nucl. Instrum. and Meth. A* 422 (1999) 368.
- [41] D. Budjaj, *et al.*, "Pulse shape discrimination studies with a Broad-Energy Germanium detector for signal identification and background suppression in the GERDA double beta decay experiment," *Journal of Instrumentation* 4 (2009) P10007.
- [42] S. E. Boggs, *et al.*, "Laboratory tests of pulse shape discrimination techniques for correcting the effects of radiation damage in germanium coaxial detectors," *Nucl. Instrum. and Meth. A* 443 (2000) 319.
- [43] S. Akkoyun *et al.*, "AGATA—Advanced GAMMA Tracking Array," *Nucl. Instrum. and Meth. A* 668 (2012) 26.
- [44] D.G. Jenkins, *et al.*, "Proof-of-principle for fast neutron detection with advanced tracking arrays of highly segmented germanium detectors," *Nucl. Instrum. and Meth. A*, Vol. 602 (2009) 457.
- [45] Th. Kroll, *et al.*, "Analysis of simulated and measured pulse shapes of closed-ended HPGe detectors," *Nucl. Instrum. and Meth. A* 371 (1996) 489.
- [46] K. F. Li and D. G. Perera, "An Investigation of chip-level hardware support for Web mining," *21<sup>st</sup> Int. Conference on Advance Information Networking and Application Workshops, (AINAW07)* 2007.
- [47] M. Freeman, M., Weeks, J. Austin, "Hardware implementation of similarity Functions," *IADIS International Conference on Applied Computing*, 2005.